

Interannual variability of ocean surface waves in the Southeast Pacific

Catalina Aguirre, Diego Becerra, Marcelo Godoy & Diego Silva

catalina.aguirre@uv.cl

Motivation

- Several global studies have shown that the interannual variability of the wave climate and the occurrence of extreme wave events are associated to large-scale climate oscillations, as the Southern Annular Mode (SAM) and El Niño Southern Oscillation (ENSO), among others (e.g. Izaguirre et al., 2011, Stopa et al., 2014, Kumar et al., 2016).
- Few studies have assessed regional wave climate in the Southern Hemisphere (e.g. Hemer et al., 2010) and the Southeast Pacific remains poorly studied.
- Recently, the first Chilean Wave Atlas database was generated and validated (Beyá et al., 2017, <https://oleaje.uv.cl/>), and the wave climatology of the Southeast Pacific was described (Aguirre et al., 2017). Nevertheless, the Southeast Pacific coast still lacks a detailed description of the interannual variability of wind waves.
- Here, we analyze the interannual variability of waves at the Southeast Pacific related to ENSO and SAM, using a model hindcast.

Datasets

MODEL DATA

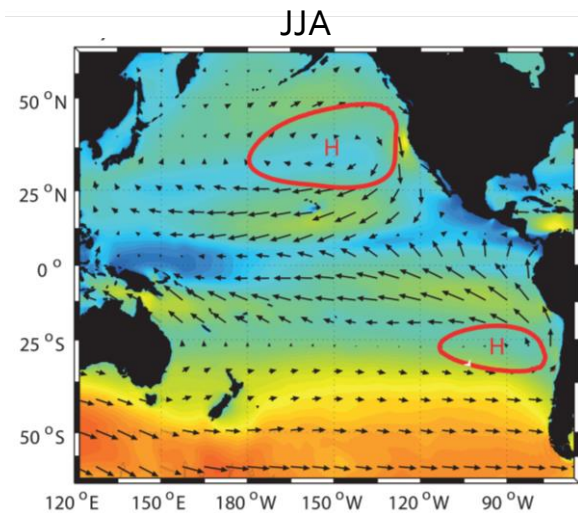
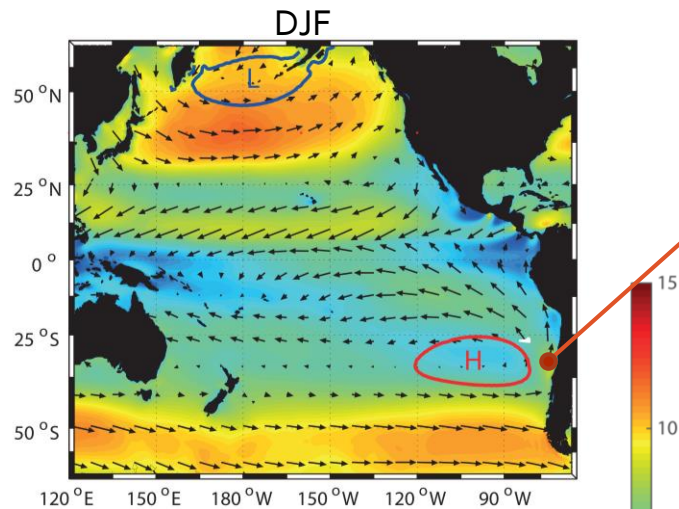
- A 38-yr hindcast was carried out for the period between 1979 and 2016 for the Pacific Ocean using the Wavewatch III v4.18
- To force the model, we used sea ice concentration and wind fields from the ECMWF atmospheric reanalysis ERA-Interim (Dee et al., 2011).
- Maps of wave parameters and spectral data along the coast of the Southeast Pacific were saved each 2° of latitude.

CICLONE TRACK

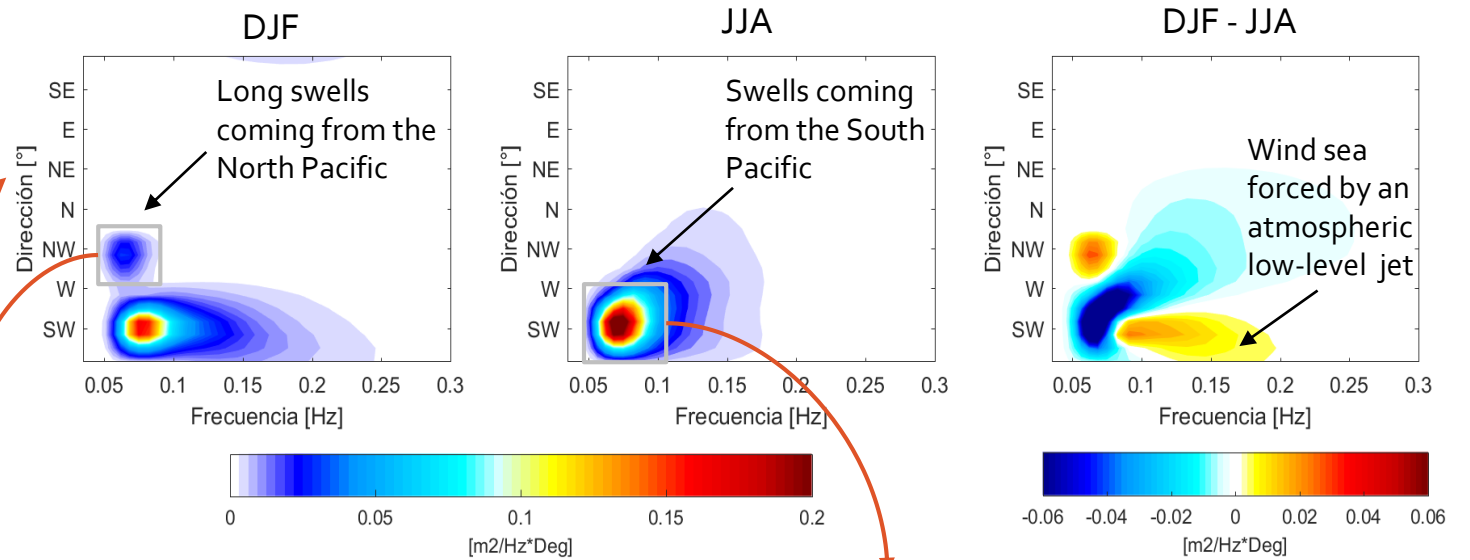
- A cyclone tracking software developed at The University of Melbourne was used (Murray and Simmonds 1991; Simmonds et al., 1999).
- Cyclones were identified using the sea level pressure data of the ERA-Interim dataset with spatial and temporal resolution of 2.5° and 6 hours, respectively.
- Sea level pressure, trajectory, duration and density of extratropical cyclones were obtained.

Seasonal Cycle

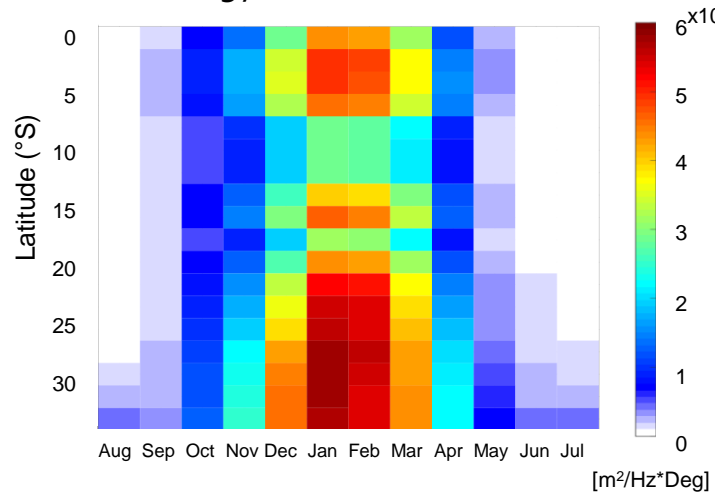
10-m Winds



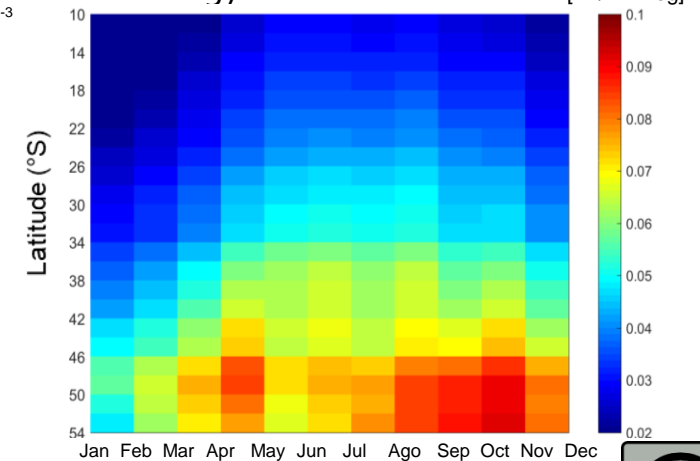
Spectrum off Valparaíso (33°S)



Energy from North Pacific

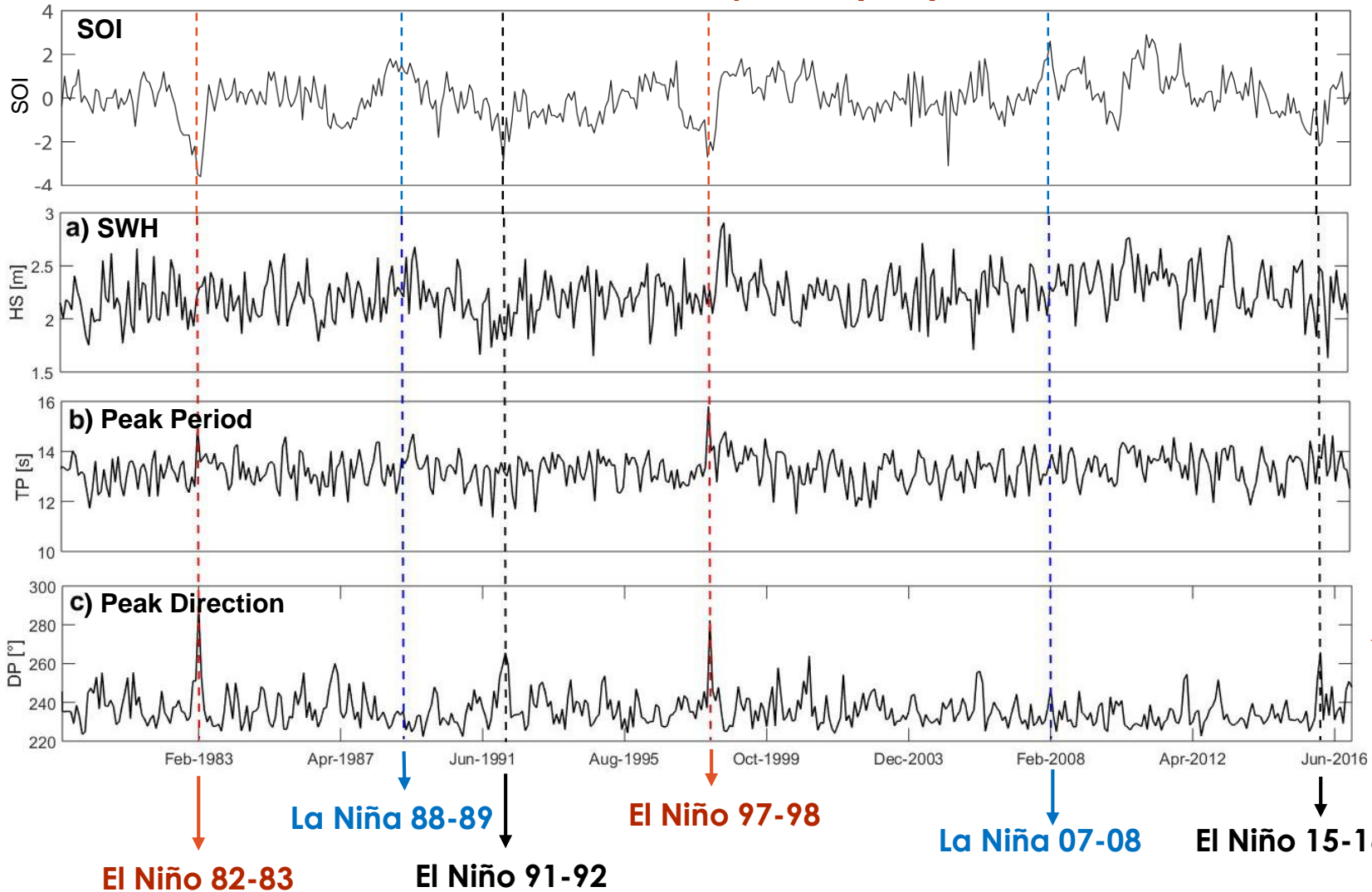


Energy from South Pacific

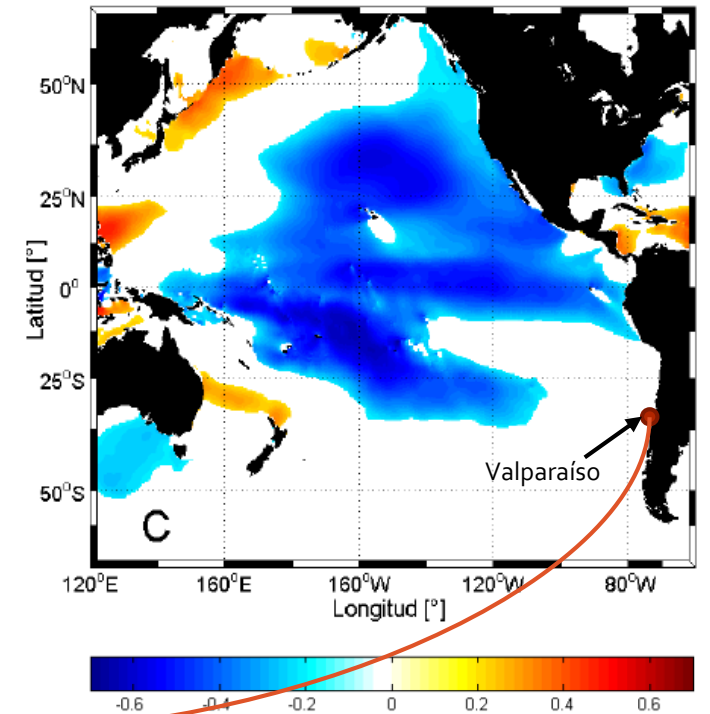


ENSO-related interannual variability of waves

Time series off Valparaíso (33°S)



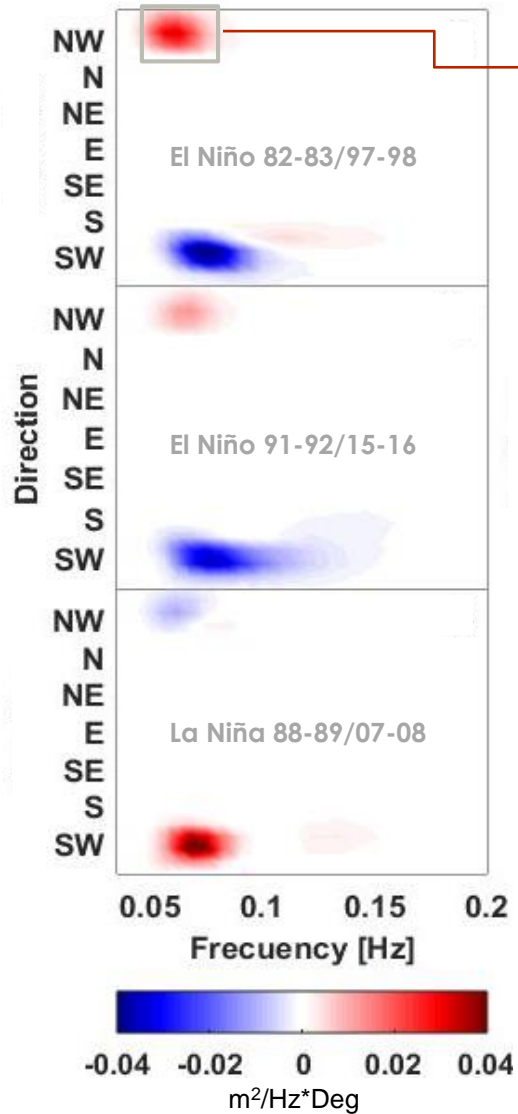
Correlation SWH-SOI



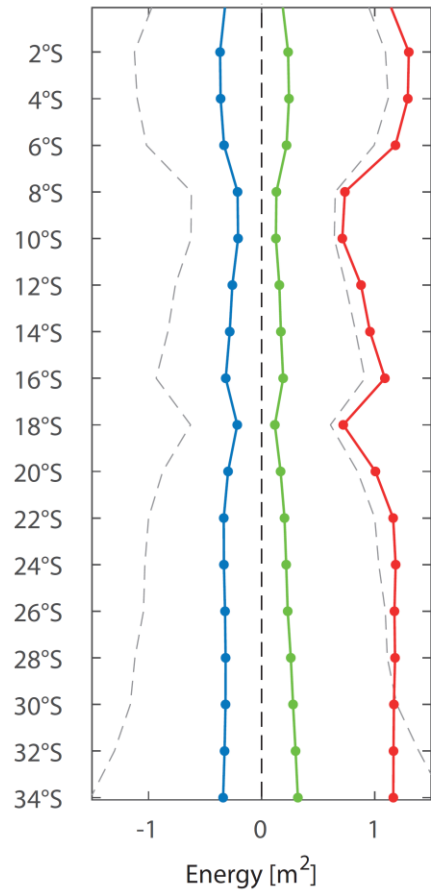
Correlation map of monthly mean SWH with the Southern Oscillation Index (SOI). Only significant correlations (at 95% confidence level) are showed.

Wave Energy anomalies

Spectrum off Valparaíso (33°S)



Energy anomalies from NW

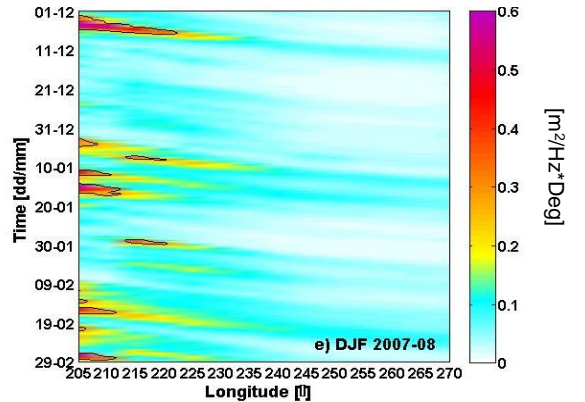
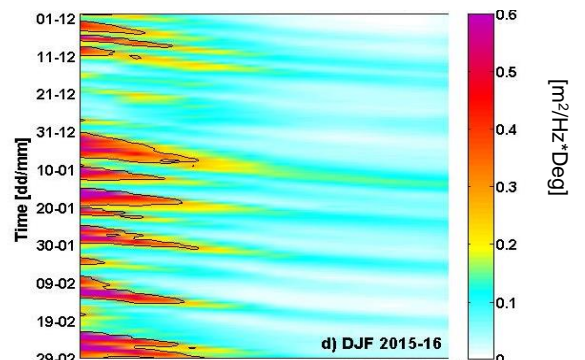
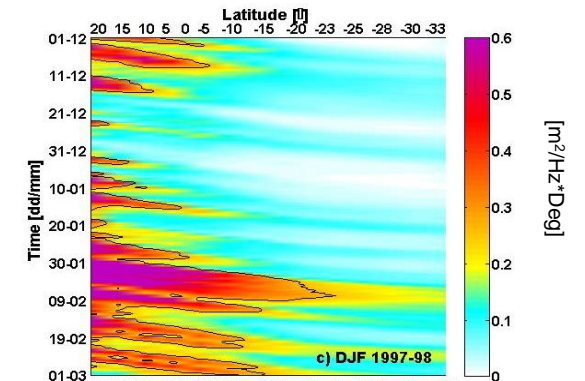
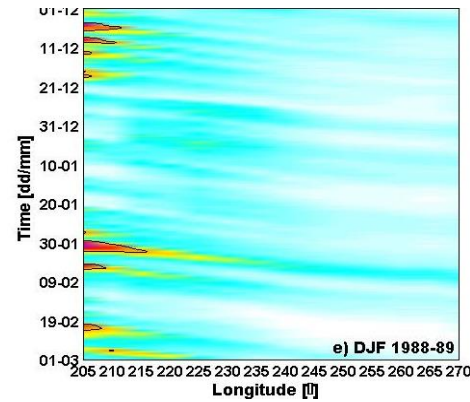
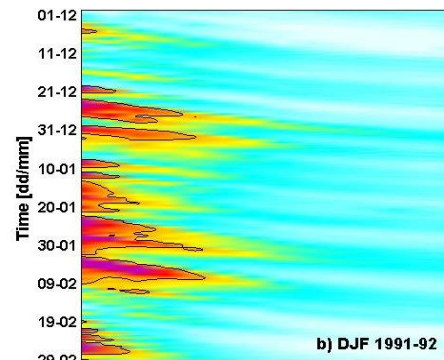
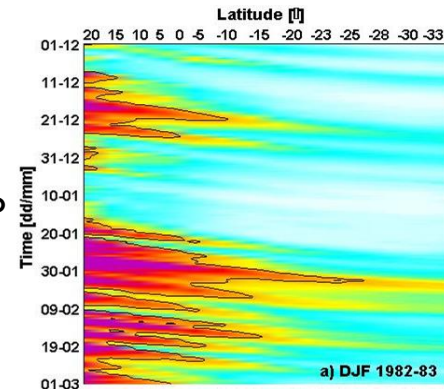


- El Niño 82-83/97-98
- El Niño 91-92/15-16
- La Niña 88-89/07-08
- Montecarlo test (90%)

Extreme El Niño

El Niño

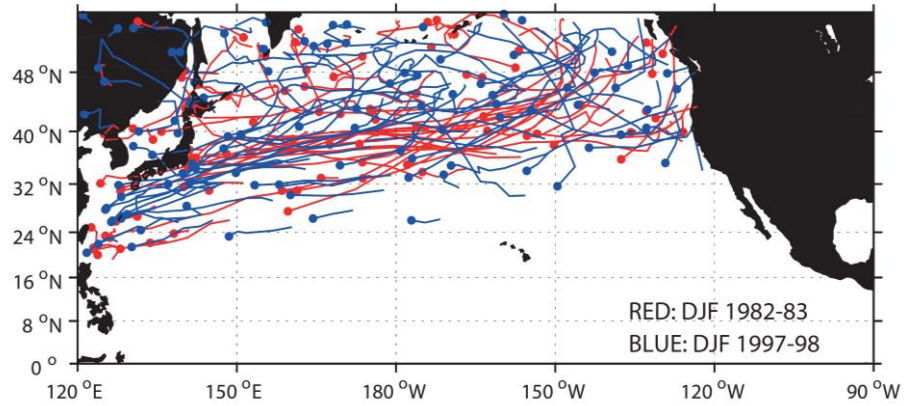
La Niña



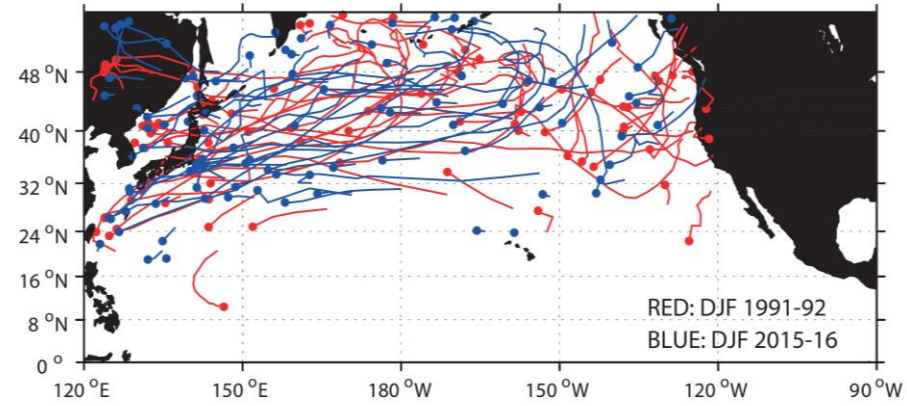
Hovmoller diagram of the wave energy with NW direction during austral summer of ENSO selected events

Cyclone Tracks

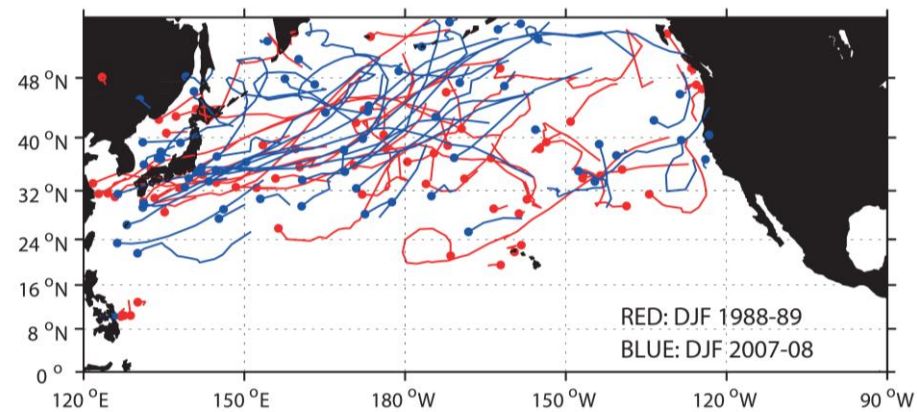
El Niño 82-83/97-98



El Niño 91-92/15-16

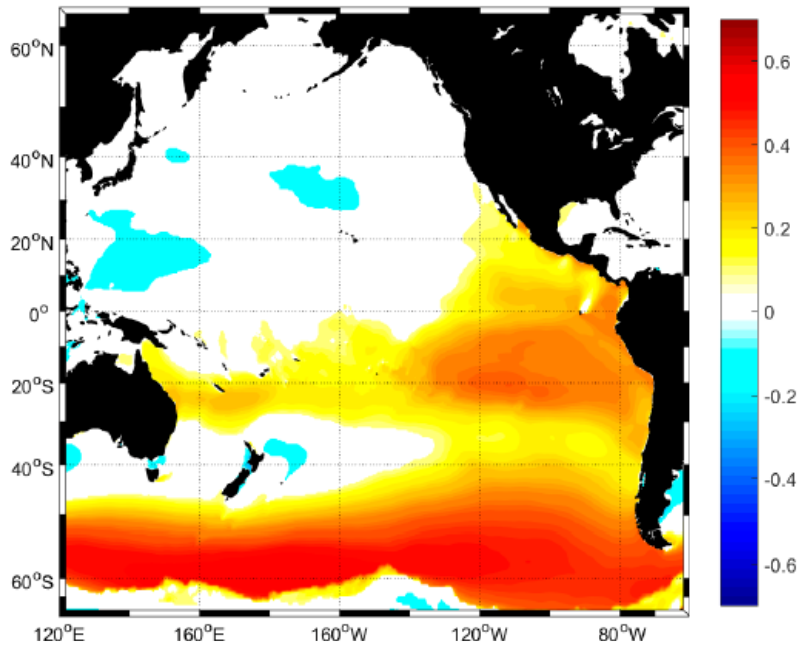


La Niña 88-89/07-08



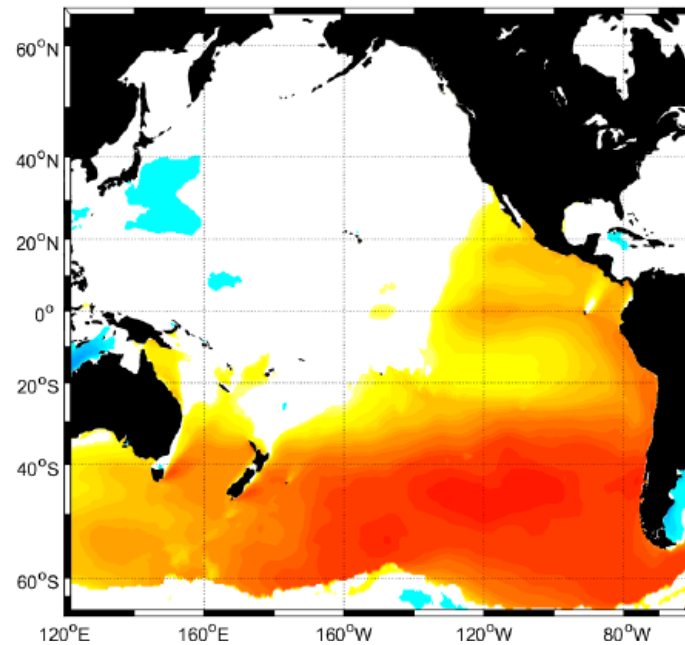
SAM-related interannual variability of waves

Correlation SWH-SAM



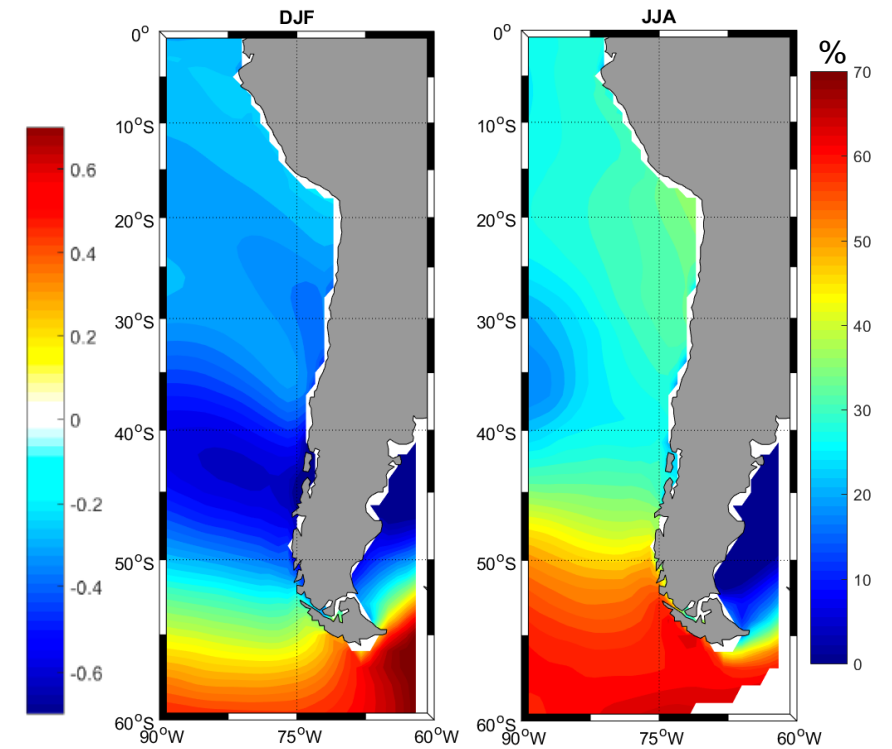
Correlation map of monthly mean SWH with the Southern Annular Mode (SAM). Only significant correlations (at 95% confidence level) are showed.

Correlation Mean period-SAM



Correlation map of monthly mean period with the Southern Annular Mode (SAM). Only significant correlations (at 95% confidence level) are showed.

Wave Power relative change



Wave power (WP) relative change calculated using the upper and lower quintiles of the SAM.

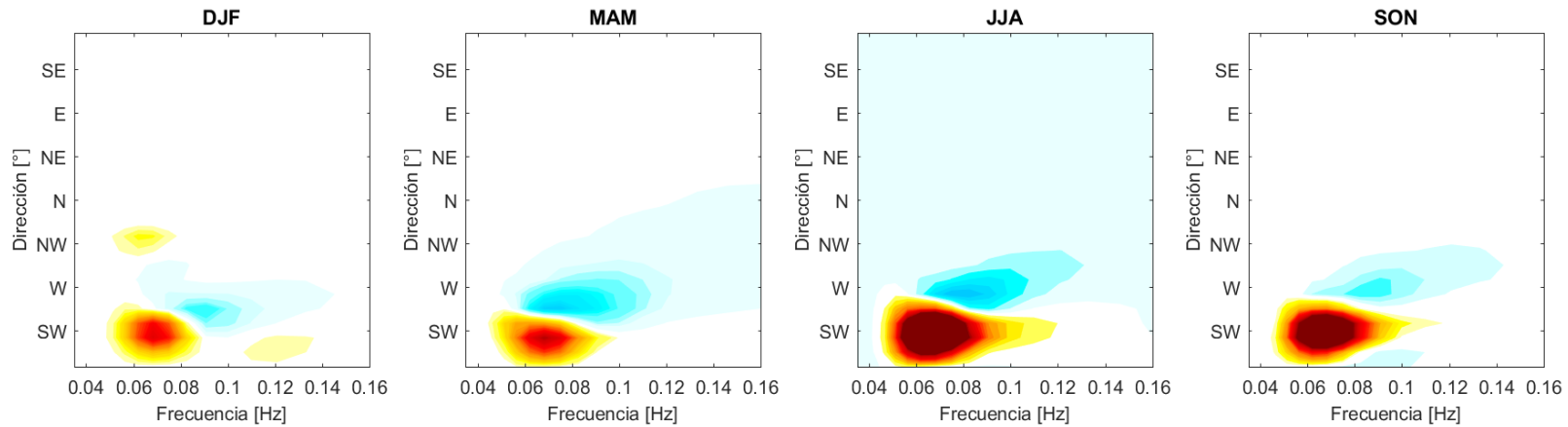
$$\frac{(WP_{SAM+} - WP_{SAM-})}{WP_{MEAN}}$$



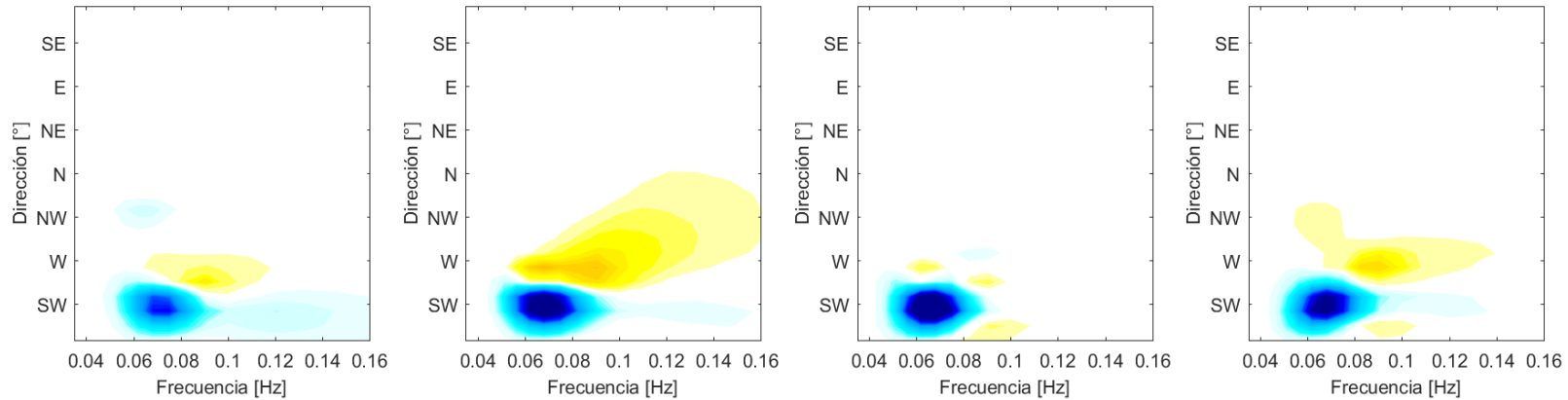
Wave Energy anomalies

Wave energy anomalies off Valparaíso (33°S)

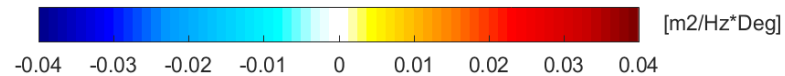
Upper quintile of the SAM
(positive phase)



Lower quintile of the SAM
(negative phase)



Composites of the wave energy calculated using the upper and lower quintiles of the SAM index.



SAM-driven SWH trends

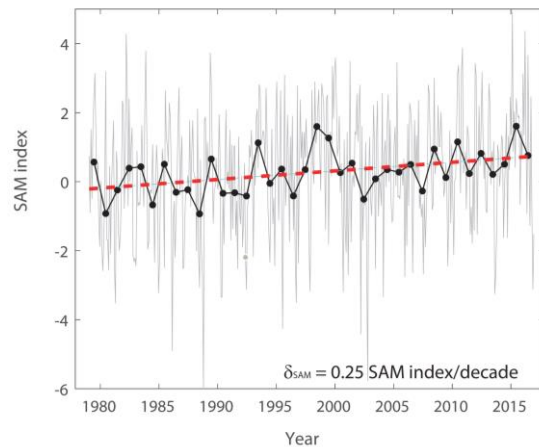
Simple linear regression framework to estimate SWH changes congruent with the SAM

The SAM-driven SWH trend is estimated as

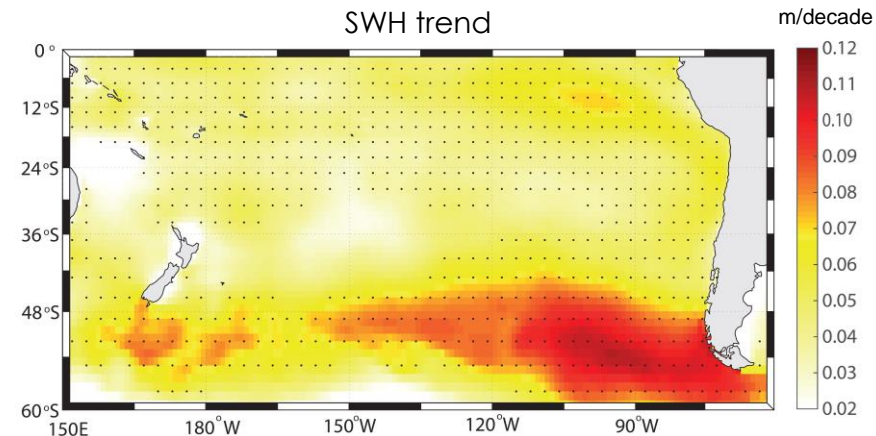
$$\delta_{\text{SWH-SAM}} = \beta \times \delta_{\text{SAM}}$$

δ_{SAM} : linear trend of the SAM index

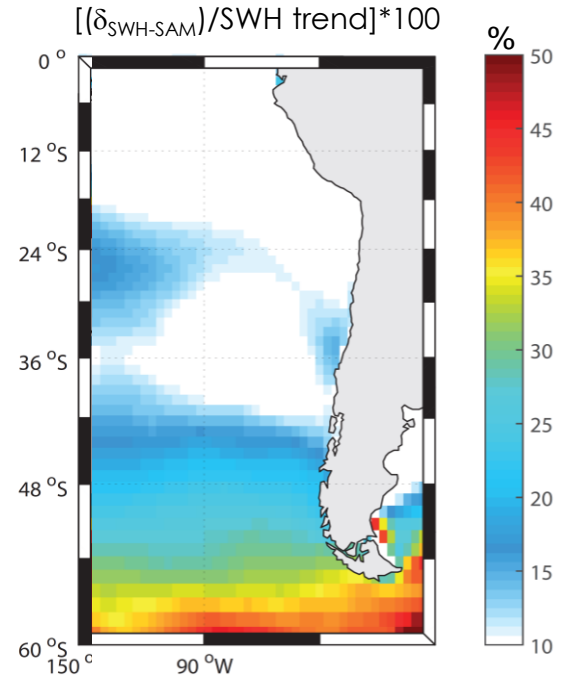
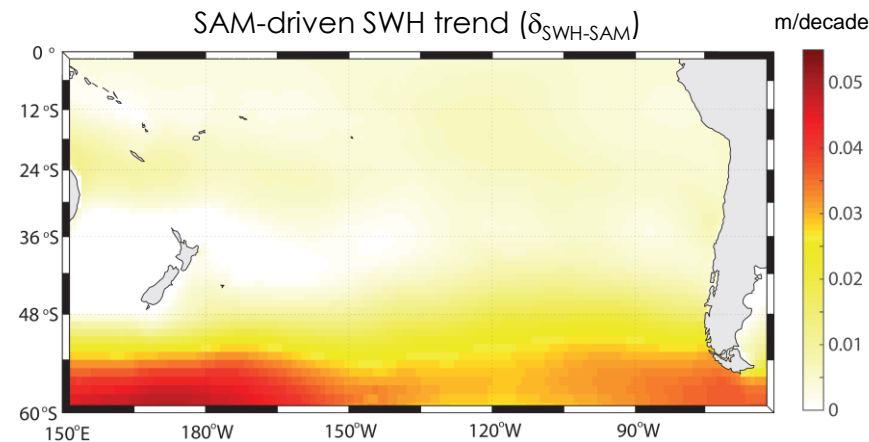
β : regression slope computed between the time series of the SAM index and simulated SWH



Time series of the SAM index (we use the index of Marshall et al. [2003], <https://legacy.bas.ac.uk/met/gjma/sam.html>)



Black dots indicate values that are statistically significant according to the Mann-Kendall test.



Over the SE Pacific, SAM-congruent SWH trend explains less than 50% of the simulated SWH trend.

Conclusions

- Although no significant relationship is found between SWH and ENSO at the Southeast Pacific, the wave energy coming from the North Pacific is significantly higher during the austral summer of the extreme ENSO events occurred during 82/83 and 97/98.
- The SWH and mean period exhibit a relationship with the SAM at the Southeast Pacific, which strongly impact the wave power, particularly at the southern tip of Chile.
- Directional spectra show an increase (decrease) of wave energy coming from SW during the positive (negative) phase of the SAM. But, spectra also indicate increased (decreased) energy coming from W-NW during the negative (positive) phase of the SAM.
- The simulated SWH shows a positive trend in the Southeast Pacific, which can be only partially attributed to the observed trend in the SAM index. While the SAM-congruent SWH trend can explain more than 50% of the simulated SWH trend in the Southern Ocean, over the Southeast Pacific, SAM-congruent SWH trend explains less than 15% of the simulated SWH trend.

References

- Aguirre, C., Rullant, J. A., & M, F. (2017). Wind waves climatology of the Southeast Pacific Ocean. *International Journal of Climatology*.
- Beyá, J., Álvarez, M., Gallardo, A., Hidalgo, H., & Winckler, P. (2017). Generation and validation of the Chilean Wave Atlas database. *Ocean Modelling*, 16-32.
- Dee, D. P., Uppala, S. M., Simmons, A. J., Berrisford, P., Poli, P., Kobayashi, S., & al., e. (2011). The ERA-Interim reanalysis: configuration and performance of the data assimilation system. *Q. J. R. Meteorol. Soc.* 137, 553–597.
- Hemer, M. A., Church, J. A., & Hunter, J. R. (2010). Variability and trends in the directional wave climate of the Southern Hemisphere. *International Journal of Climatology* , 475-491.
- Izaguirre, C., Méndez, F. J., Menéndez, M., & Losada, I. J. (2011). Global extreme wave height variability based on satellite data. *Geophysical research Letters* , 38(L10607, doi:10.1029/2011GL047302.), 1-6.
- Kumar, P., Min, S.-K., Weller, E., Lee, H., & Wang, X. L. (2016). Influence of Climate Variability on Extreme Ocean Surface Wave Heights Assessed from ERA-Interim and ERA-20C. *American Meteorological Society*, 4031-4045.
- Marshall GJ. 2003. Trends in the Southern Annular Mode from observations and reanalyses. *Journal of Climate*, 16: 4134–4143
- Murray, R., & Simmonds, I. (1991). A numerical scheme for tracking cyclone centres from digital data. Part I: Development and operation of the scheme . *Aust. Meteorol. Mag.* 39, 155-166.
- Stopa, J. E., & Cheung, K. F. (2014). Periodicity and patterns of ocean wind and wave climate. *Journal of Geophysical Research: Oceans* , 5563-5584.F

Funding

- FONDECYT N°11171163
- FONDAP N°15110009